Solvation shell dynamics studied by molecular dynamics simulation in relation to the translational and rotational dynamics of supercritical water and benzene

Ken Yoshida, Nobuyuki Matubayasi,[a),b)] and Masaru Nakahara[a),c)]
Institute for Chemical Research, Kyoto University, Uji, Kyoto 611-0011, Japan

The solvation shell dynamics of supercritical water is analyzed by molecular dynamics simulation with emphasis on its relationship to the translational and rotational dynamics. The relaxation times of the solvation number (τ^S), the velocity autocorrelation function (τ^D), the angular momentum correlation function (τ^J), and the second-order reorientational correlation function (τ^{2R}) are studied at a supercritical temperature of 400 °C over a wide density region of $0.01-1.5$ g cm^{-3}. The relaxation times are decomposed into those conditioned by the solvation number n, and the effect of the short-ranged structure is examined in terms of its probability P_n of occurrence. In the low to medium-density range of $0.01-0.4$ g cm^{-3}, the time scales of water dynamics are in the following sequence: $\tau^D > \tau^S \gtrsim \tau^J \gtrsim \tau^{2R}$. This means that the rotation in supercritical water is of the "in-shell" type while the translational diffusion is not. The comparison to supercritical benzene is also performed and the effect of hydrogen bonding is examined. The water diffusion is not of the in-shell type up to the ambient density of 1.0 g cm^{-3}, which corresponds to the absence of the transition from the collision to the Brownian picture, whereas such transition is present in the case of benzene. The absence of the transition in water comes from the fast reorganization of the hydrogen bonds and the enhanced mobility of the solvation shell in supercritical conditions. © *2007 American Institute of Physics*. [DOI: 10.1063/1.2780871]

I. INTRODUCTION

Supercritical water has received much attention as a clean and novel alternative to organic solvents.[1–7] The dynamics of hydration often plays an important role in determining the reaction rate constant, how long it takes for reactive species to encounter each other, how long molecules reside in a solvation shell, and how long reactive orientation persists. The dynamics of supercritical aqueous solution is inseparably related to the dynamical structure of pure solvent water at the supercritical state. Thus, in order to establish the molecular picture of the supercritical hydration dynamics, it is essential to elucidate the dynamics of supercritical water as a pure solvent.

In previous papers, we have investigated the self-diffusion and the rotational relaxation of sub- and supercritical water over a wide range of temperature (30–400 °C) and density (0.004–1.0 g cm^{-3}) using the high-temperature nuclear magnetic resonance (NMR) method.[8–10] The effect of the hydrogen bonding on the self-diffusion has been elucidated in terms of the simple gas kinetic model[11–13] and the simple hydrodynamic model.[14,15] The experimental results alone cannot give a full account of the self-diffusion mechanism on the molecular level, however, since the microscopic details are averaged out in the integral of the relevant time correlation function. The molecular dynamics (MD) method

is a complementary, powerful tool to analyze the dynamics at the atomic spatial resolution and femto- to picosecond time resolution.[8–10,16–25] Its numerical results can be combined with an analytical formulation to provide a realistic, physical picture, which is often missed in widely used models such as the binary collision and Brownian dynamics. The purpose of the present work is to pursue the solvation shell picture in connection to the dynamics of supercritical water. We aim at obtaining a deeper understanding of the molecular mechanism of the translational and rotational dynamics in terms of the time correlation functions obtained by computer simulation.

Since the time profiles of the velocity and the orientation in fluids are controlled by the forces exerted by solvating molecules, it is of great interest to establish the relationship between the dynamics and the solvating shell structures over a wide range of density. One of our purposes is to see whether or not the supercritical water dynamics is of the "in-shell" type in the sense that a water molecule diffuses or rotates within the "shell" or "cage" of solvating molecules clustering around it.[26] For this purpose, it is necessary to explore the dynamic aspect of the shell structure as well as the static one. In supercritical water, the hydrogen bonding is still present,[18,21] and thus the attractive intermolecular interaction is important in the translational and rotational dynamics. Previously, by characterizing the attractive effect by the number n_{HB} of hydrogen bonds, we have analyzed the rotational correlation time τ^{2R} for supercritical water in relation to n_{HB} and have shown that τ^{2R} is dominantly controlled by the local hydrogen-bonding structure.[8] τ^{2R} has also been

found to be smaller than the angular momentum relaxation time τ^J in supercritical states, showing that the inertial effect is operative. There have also been studies on the dynamics of each individual hydrogen bond in water and aqueous solutions in ambient and supercritical conditions.[27–31] In this study, we extend our focus to the observable translational and rotational dynamics and establish the relationship among the relaxations of collective shell structure, velocity, orientation, and angular momentum over a wide range of density.

To clarify the effect of the hydrogen-bonding interaction, it is beneficial to compare the simulation results for water and those for a solvent without hydrogen bonding, such as benzene. A comparison to benzene will provide a better understanding of dynamical issues in supercritical fluids that have generated considerable interest during the past decades.[32–43] Although the structure and dynamics in benzene are slightly anisotropic at room temperature,[44,45] the anisotropy is much weaker than in water, especially at high temperatures.[45] The studies on static structures have shown that the preference for parallel and perpendicular configurations in benzene almost disappears in supercritical conditions,[45] whereas the orientational preference in hydrogen bonding clearly exists in supercritical water.[21] Thus the comparison between water and benzene enables us to highlight the effect of the strongly anisotropic pair potential of water. In particular, the rotational dynamics is a powerful probe to examine the effect of short-ranged, anisotropic interactions and is to be treated in detail.[46–48] It is furthermore interesting to see to what extent benzene can be considered to be freely rotating in supercritical conditions. Thus we compare the results for benzene with those for the Lennard-Jones (LJ) fluid.

This paper is organized as follows. Section II describes the procedures for the MD simulation and the summary of the time correlation functions and relaxation times examined. Section III is devoted to the analysis of the shell structure and shell relaxation dynamics in connection to the translational and the rotational dynamics. Conclusions are given in Sec. IV.

II. METHODS

A. Molecular dynamics simulation

The MD simulation was performed for pure water and benzene. The supercritical states simulated in the present work are specified by a temperature of 400 °C and for water by densities of 0.01, 0.02, 0.05, 0.10, 0.20, 0.40, 0.60, 1.0, 1.2, and 1.5 g cm^{-3} and for benzene by densities of 0.01, 0.02, 0.05, 0.10, 0.20, 0.40, 0.60, and 0.87 g cm^{-3}. These densities correspond to the reduced densities, $\rho_r = \rho/\rho_c$, of 0.031, 0.062, 0.16, 0.31, 0.62, 1.24, 1.86, 3.11, 3.73, and 4.66 for water and 0.033, 0.066, 0.16, 0.33, 0.66, 1.31, 1.97, and 2.86 for benzene, respectively, where ρ_c is the critical density. The experimental ρ_c values are equal to 0.322 and 0.305 g cm^{-3} for water[49] and benzene,[50] respectively, and they were used in the above-mentioned conversions. To examine the temperature effect, we also studied an ambient state: 30 °C and 1.0 g cm^{-3} for water and 30 °C and 0.87 g cm^{-3} for benzene. The water density is covered up to

1.5 g cm^{-3} in order to compare water and benzene at high molecular packing fractions; the packing fraction, $(4\pi/3)\rho_n(\sigma/2)^3$, is 0.48 at 1.5 g cm^{-3} for water and is 0.51 at 0.87 g cm^{-3} for benzene, where ρ_n is the number density and σ is the molecular diameter. The σ values of 2.64 and 5.27 Å are used for water and benzene, respectively. These σ values are taken from the LJ parameters in Refs. [11] and [51] for benzene and water, respectively. Note that the packing fraction for water is only 0.32 at 1.0 g cm^{-3} due to the open structure.[1]

The water and benzene molecules were treated as rigid and nonpolarizable. The TIP4P (Ref. [52]) and OPLS-AA (Ref. [53]) models were adopted as the potential functions for water and benzene, respectively. As a reference solvent that has a completely isotropic potential, the LJ fluid was also simulated. The potential parameters for the LJ fluid were set to $\sigma = 5.27$ Å and $\varepsilon/k_B = 440$ K.[11] These are optimized ones for benzene using the viscosity data.[11] The pairwise additivity was assumed, and the Lennard-Jones and Coulombic interactions were operative between a pair of sites belonging to different molecules. The standard Lorentz-Berthelot combining rule was used to construct the Lennard-Jones part of the interaction between different types of sites.[54] The number of molecules in the unit cell was 1000, 256, and 1000 for water, benzene, and LJ fluid, respectively. The periodic boundary condition was employed with the minimum image convention, and the electrostatic potential was handled by the Ewald method with the surrounding medium of infinite dielectric constant.[55] The equations of motion were integrated at a time step of 1.0 fs. The simulation was performed for 1.0 ns at low densities to determine the relatively large relaxation time ($\lesssim 10$ ps) associated: in the case of water, for the translational dynamics at the densities of 0.1 g cm^{-3} and lower and for the angular momentum dynamics at 0.05 g cm^{-3} and lower. In the case of benzene, a 1.0 ns simulation was performed for the translational dynamics at 0.2 g cm^{-3} and lower and for the angular momentum dynamics at 0.05 g cm^{-3} and lower. At the higher densities, the MD was conducted for 100 ps to see the relatively fast relaxation ($\lesssim 1$ ps) for the translational, the shell, and the rotational dynamics. The errors of the calculated relaxation times are within ±2%. Those of the decomposed (solvation-number-conditioned) relaxation times are within ±5% for the solvation numbers with which the P_n is larger than 0.01, where P_n is the probability of finding a molecule with the solvation number equal to n; the shell decomposition scheme is described in Sec. II B. Such small errors do not affect the physical contents below. The MD calculations were performed by using MATERIALS EXPLORER 4.0 (Fujitsu Ltd.).

B. Shell decomposition of the time correlation function

In order to characterize the local states of the solvating molecules, we employ the solvation number n as a variable. The solvation number is well suited for the comparison of dynamics between water and benzene. The solvation number is defined for water and benzene in terms of the distance of the center of mass of a pair of molecules. For a given molecule, its solvation number n is equal to the number of mol-

ecules whose distances are less than a cutoff distance r_c. The cutoff distance r_c was taken to be 5.0 and 9.0 Å for water and benzene, respectively, and corresponds approximately to the first minimum of the radial distribution function of the center of mass. Since the position of the first minimum is less clear in supercritical conditions, we also used r_c =4.0 Å for water and 8.0 and 10.0 Å for benzene to confirm that the discussions are not altered by the choice of r_c. For brevity the results are shown only for the r_c values of 5.0 and 9.0 Å, respectively, for water and benzene.

The dynamics of the solvation shell structure is investigated through a characteristic function, $\Theta_n(t)$, of the solvation number. At time t, this function is unity when the solvation number is equal to n and is zero otherwise. $\Theta_n(t)$ satisfies

$$\Theta_m(t)\Theta_n(t) = \Theta_n(t) \quad (m = n)$$

$$= 0 \quad (m \neq n), \tag{1}$$

$$\sum_n \Theta_n(t) = 1 \tag{2}$$

at any time t. In this definition, $\Theta_n(t)$ picks up the information only at time t and does not reflect whether an exchange of solvating molecules occurs between time 0 and t. The normalized autocorrelation function $C_n(t)$ for Θ_n is expressed as

$$C_n(t) = \frac{\langle \Theta_n(t)\Theta_n(0)\rangle}{\langle \Theta_n^2 \rangle} = \frac{\langle \Theta_n(t)\Theta_n(0)\rangle}{\langle \Theta_n \rangle}. \tag{3}$$

The second equality comes from the definition that Θ_n is either zero or unity. $C_n(t)$ is unity at time 0 and decays to the ensemble average $\langle \Theta_n \rangle \equiv \langle \Theta_n(0)\rangle$. The average $\langle \Theta_n \rangle$ is the probability P_n of finding a molecule with the solvation number equal to n. In the present study, the relaxation time τ_n^S was calculated by an exponential fit of the initial decay of $C_n(t)$; the initial part here refers to the t region in which $C_n(t) \geqslant 0.7$ (no n with $\langle \Theta_n \rangle \geqslant 0.7$ was found), except for n =0 at 0.01 g cm^{-3} where the t region in which $C_n(t) \geqslant 0.9$ is used. The average of τ_n^S over n is the relaxation time τ^S at a specific thermodynamic state expressed as

$$\tau^S = \sum_n \langle \Theta_n \rangle \tau_n^S = \sum_n P_n \tau_n^S. \tag{4}$$

The self-diffusion coefficient D was calculated by integrating the velocity autocorrelation function of the center of mass through

$$D = \frac{1}{3}\int_0^\infty dt \langle \mathbf{v}(0) \cdot \mathbf{v}(t)\rangle. \tag{5}$$

The relaxation time τ^D of the velocity autocorrelation function is calculated by integrating the normalized velocity autocorrelation function as

$$\tau^D = \int_0^\infty dt \frac{\langle \mathbf{v}(0) \cdot \mathbf{v}(t)\rangle}{\langle \mathbf{v}(0)^2 \rangle}. \tag{6}$$

τ^D is directly related to D by

$$\tau^D = \frac{M}{RT}D, \tag{7}$$

where M is the molecular weight, R is the gas constant, and T is the temperature.

The rotational dynamics is investigated in terms of the angular momentum correlation time τ^J and the second-order reorientational correlation time τ^{2R}, described, respectively, as

$$\tau^J = \int_0^\infty dt \frac{\langle \mathbf{J}(0) \cdot \mathbf{J}(t)\rangle}{\langle \mathbf{J}(0)^2 \rangle}, \tag{8}$$

$$\tau^{2R} = \int_0^\infty dt \langle \tfrac{3}{2} \cos^2 \theta(t) - \tfrac{1}{2}\rangle, \tag{9}$$

where $\mathbf{J}(t)$ is the angular momentum vector of a molecule at time t and $\theta(t)$ is the angle between the O–H and C–H bond vectors for water and benzene, respectively, at time 0 and t.

The dependence of τ^D, τ^J, and τ^{2R} on the solvation number is examined through the corresponding correlation functions conditioned by n at time 0. τ^D, τ^J, and τ^{2R} conditioned by Θ_n are expressed, respectively, as

$$\tau_n^D = \int_0^\infty dt \frac{\langle \mathbf{v}(0)\mathbf{v}(t)\Theta_n(0)\rangle}{\langle \mathbf{v}(0)^2 \Theta_n(0)\rangle}, \tag{10}$$

$$\tau_n^J = \int_0^\infty dt \frac{\langle \mathbf{J}(0)\mathbf{J}(t)\Theta_n(0)\rangle}{\langle \mathbf{J}(0)^2 \Theta_n(0)\rangle}, \tag{11}$$

$$\tau_n^{2R} = \int_0^\infty dt \frac{\langle ((3/2)\cos^2 \theta(t) - 1/2)\Theta_n(0)\rangle}{\langle \Theta_n(0)\rangle}. \tag{12}$$

The averages of τ_n^D, τ_n^J, and τ_n^{2R} over n give τ^D, τ^J, and τ^{2R}, respectively, by

$$\tau^D = \sum_n P_n \tau_n^D, \tag{13}$$

$$\tau^J = \sum_n P_n \tau_n^J, \tag{14}$$

$$\tau^{2R} = \sum_n P_n \tau_n^{2R}. \tag{15}$$

Equations (13)–(15) are "sum rules" in our description by the solvation number. The observable quantities τ^D, τ^J, and τ^{2R} are expressed as weighted sums of their components conditioned by the solvation number n. The weight is the probability P_n of finding a specific value of n at time 0, and the time evolution with the specific n determines the components. This decomposition scheme is exact over the entire density region and does not rely on any specific dynamic model.

C. Physical concepts based on conditional correlation time

In the present formalism, we can obtain a dynamic picture in supercritical fluids on the basis of the relaxation time τ_n^X of the dynamics of interest ($X = D$, J, or $2R$) divided by the

shell relaxation time τ_n^S. The condition $\tau_n^X/\tau_n^S < 1$ shows that the dynamic mode of interest is randomized through intermolecular interactions within the solvation shell. In this case, the dynamics is relatively confined within the shell and classified into the in-shell type. The opposite condition $\tau_n^X/\tau_n^S > 1$ shows that the autocorrelation persists after the initial shell state is relaxed. Expressed in another way, the shell relaxation is relatively faster. The shell relaxation occurs when a solvent molecule escapes out of or enters into the shell, and therefore the faster shell relaxation indicates that the shell is more "mobile." The dynamics of the mobile-shell type relaxes through repeated reorganization of temporary shells. The former in-shell type is more local in time and the latter mobile-shell type is more nonlocal.

Our approach is valid over a wide range of density from dilute gas to liquid. The two extremes of time scale separation, $\tau_n^X/\tau_n^S \gg 1$ and $\tau_n^X/\tau_n^S \ll 1$, correspond to dilute gas and dense liquid, respectively, for velocity and angular momentum relaxations ($X = D$ and J). As for the self-diffusion in dilute gas, the velocity correlation will be lost after repeated binary collisions (interactions)[56] and thus τ^D/τ^S can be large. At liquidlike high densities, the solute molecule is subject to fluctuating forces and torques from various directions within a somewhat packed shell and hence τ^D/τ^S can be small. A larger and a smaller value of τ_n^D/τ_n^S are in favor of the binary collision picture and the Brownian picture, respectively. The present formalism is useful for assessing the validity and limitations of these popular pictures. By examining τ_n^X/τ_n^S, we can discuss to what extent the fluid dynamics deviates from the binary collision or the Brownian depending on the density region.

How much a certain dynamic mode relaxes within the shell or not determines how strongly the dynamic mode is controlled by the shell structure. To see this point, in Sec. III we will discuss τ_n^X in terms of its dependencies on the solvation number n and the bulk density ρ; at each fixed ρ, τ_n^X is a function of n and at each n, the ρ dependence can be assessed since ρ is to be varied to study supercritical fluid. Here we summarize the general correlation between the ratio τ_n^X/τ_n^S and the relative strength of the dependencies of τ_n^X on n and ρ. When τ_n^X/τ_n^S is smaller than unity (in-shell type), τ_n^X is dominantly determined by the integral from $t=0$ to $\sim \tau_n^S$. Within the time scale of τ_n^S, the majority of molecules keep the n value at time 0. Thus τ_n^X is strongly controlled by the solvation number n. In the opposite case that τ_n^X/τ_n^S is larger than unity (mobile-shell type), the integral τ_n^X is the sum of the integral from $t=0$ to $\sim \tau_n^S$ (in-shell relaxation) and the integral beyond $\sim \tau_n^S$. In general, the initial period between $t=0$ and $\sim \tau_n^S$ is strongly controlled by n. After $\sim \tau_n^S$, however, the initial memory of the solvation number n is lost and thus the n dependence becomes weaker. When the shell is more mobile and the dynamics is less local in time, the n dependence is relatively weaker and the ρ dependence appears relatively more strongly. We shall see in the following sections that the dynamics of the in-shell type is more strongly controlled by n and less by ρ. On the contrary, the dynamics of the mobile-shell type will be controlled both by n and ρ.

Our dynamic analysis based on Eqs. (13)–(15) is parallel in spirit to the solvation shell analysis of partial molar thermodynamic quantities developed in Refs. 57–59. In both of the analysis schemes, the observable quantity is exactly formulated to be a weighted sum of its components conditioned by a static and spatial distribution of solvent molecule. The components then carry information specific to the observable of interest, and the exact sum rule is used to analyze the validity and limitations of a corresponding, phenomenological model on the molecular level.

III. RESULTS AND DISCUSSION

A. Solvation shell dynamics

Before discussing the dynamics of the solvation shell, we examine the static solvation shell structure over a wide range of thermodynamic conditions. In Figs. 1(a) and 1(b), the P_n distribution is shown at 400 °C for supercritical water at 0.05–1.0 and 0.01–0.02 g cm^{-3}, respectively. It is seen that the distribution mode of P_n shifts to a lower value of n with density reduction.

We first shed light on the gaslike behavior from the static viewpoint based on the P_n distribution. The gaslike behavior is characterized by the condition where a molecule is categorized into either $n=0$ (free translation) or $n=1$ (during binary interaction) and P_n at $n \geq 2$ is negligible. In Figs. 1(a) and 1(b), it is seen that such a gaslike condition is not attained until the density is decreased down to the lowest density of 0.01 g cm^{-3}. At 0.01 g cm^{-3}, P_n at $n \geq 2$ is negligibly small. Even at such a low density of 0.01 g cm^{-3}, however, P_1 is not negligible (~ 0.2). The dilute-gas condition, $P_0 \simeq 1$, is attained at one order of magnitude lower density; P_0 is estimated to be 0.98 at 0.001 g cm^{-3} from the previous simulation results in the extremely low-density region.[10] At densities higher than 0.01 g cm^{-3}, not the isolated binary but the collective, continuous intermolecular interaction is important. Even at a low density of 0.05 g cm^{-3}, one order of magnitude lower than the critical, P_0 and P_1 are only 0.3 and 0.35, respectively, and the sum of P_n at $n \geq 2$, representing the trimer and larger, is as large as 0.35.[60] Later we shall examine the gaslike behavior on the basis of the solvation shell dynamics. In the case of water, hydrogen bonding can also be used to define the solvation shell.[8–10,18,21] In Figs. 1(c) and 1(d), we show the probability $P_{n\mathrm{HB}}$ of finding a molecule with the number of hydrogen bonding equal to n_{HB}. Here we define n_{HB} by counting the pair of water molecules whose closest O–H distance is less than a cutoff distance, 2.4 Å. This cutoff distance corresponds approximately to the first minimum of the site-site radial distribution function of the O–H pair and the n_{HB} counting is done only in terms of the O–H distance irrespective of the hydrogen-bond angle. The $P_{n\mathrm{HB}}$ distribution has a maximum at $n_{\mathrm{HB}} \simeq 4$ at the ambient density of 1.0 g cm^{-3} and the distribution mode of $P_{n\mathrm{HB}}$ shifts to a lower value of n_{HB} with decreasing density. The above-mentioned trend of the P_n distribution is also common to benzene as shown in Figs. 1(e) and 1(f).

In order to focus on the deviation of the local density of the solvating molecules from the bulk one, we show in Fig. 1(g) the average $\langle n \rangle$ divided by the bulk density ρ against ρ. In fact, $\langle n \rangle/\rho$ is the average of the radial distribution function
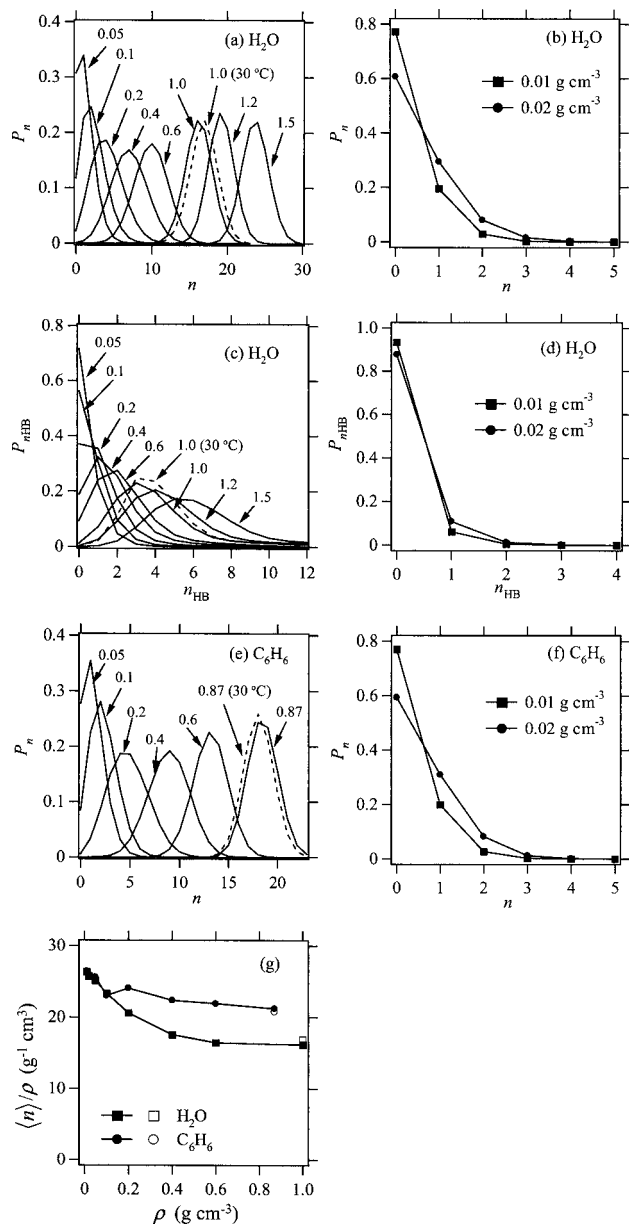
FIG. 1. The probability P_n of finding a molecule with n other surrounding molecules for water (a) at $0.05-1.5$ g cm^{-3} and (b) at 0.01 and 0.02 g cm^{-3}; the probability P_{nHB} of finding a molecule with n_{HB} for water (c) at $0.05-1.5$ g cm^{-3} and (d) at 0.01 and 0.02 g cm^{-3}; P_n for benzene (e) at $0.05-0.87$ g cm^{-3} and (f) at 0.01 and 0.02 g cm^{-3}. The solid and dashed lines in (a), (c), and (e) represent P_n and P_{nHB} at a supercritical temperature of 400 °C and at an ambient state, respectively. The numbers in (a), (c), and (e) represent the bulk density ρ in the unit of g cm^{-3}. (g) The average of the solvation number divided by the bulk density $\langle n \rangle / \rho$ as a function of the bulk density ρ. Open symbols represent the values at an ambient state.

of the center of mass over the region defined by the cutoff distance r_c. It is seen that $\langle n \rangle / \rho$ for water increases with density reduction, in agreement with previous NMR chemical shift measurements.[18,21] This shows that a specific attractive interaction between a pair of water molecules is stronger at a lower density, being less perturbed by directional collective interactions. In contrast, an increase in $\langle n \rangle / \rho$ for benzene with density reduction is weaker than that for water, corresponding to the weaker density dependence of the radial distribution function for benzene.
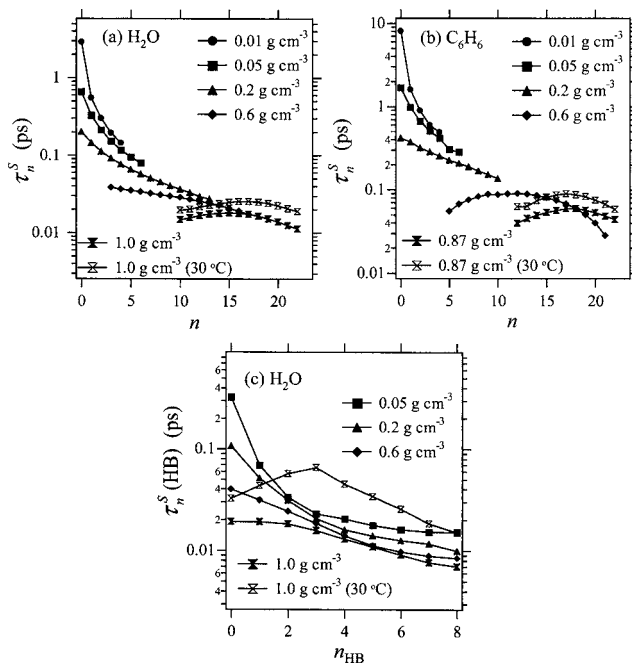
Now we discuss the dynamics of the solvation shell. In

FIG. 2. The relaxation time τ_n^S of the solvation shell as a function of the solvation number n; (a) water at supercritical states of $0.01-1.0$ g cm^{-3} and 400 °C and at an ambient state of 1.0 g cm^{-3} and 30 °C and (b) benzene (OPLS-AA) at supercritical states of $0.01-0.87$ g cm^{-3} and 400 °C and at an ambient state of 0.87 g cm^{-3} and 30 °C. (c) τ_n^S(HB) of water conditioned by the number n_{HB} of hydrogen bonding as a function of n_{HB}. The filled and open symbols represent τ_n^S at a supercritical temperature of 400 °C and at an ambient state, respectively. For each n and n_{HB}, the data at supercritical states correspond to the bulk densities of (a) $0.01-1.0$ g cm^{-3}, (b) $0.01-0.87$ g cm^{-3}, and (c) $0.05-1.0$ g cm^{-3} from top to bottom.

Fig. 2(a), we show the shell relaxation time τ_n^S for water conditioned by the solvation number n as in Eq. (4). τ_n^S at fixed n increases with decreasing ρ and τ_n^S at fixed ρ increases with decreasing n. The shell state for a more crowded shell relaxes faster due to the more frequent exchange of the solvating molecules. In order to scrutinize the effect of hydrogen bonding, we compare τ_n^S for water with that for benzene that has no hydrogen bonding. As shown in Fig. 2(b), the shell relaxation of benzene is more directly related to ρ and less to n than that of water. The larger n dependence, which is observed in the case of water, is an indication of the effect of attractive interaction.

The conditional shell relaxation time τ_n^S is a measure to assess the extent of the gaslike character of a particular supercritical state. In gaslike conditions, the time spent on free translation (τ_0^S) becomes relatively longer than that for collision or interaction $[\tau_n^S(n \geq 1)]$. Thus a larger value of the ratio τ_0^S / τ_n^S ($n \geq 1$) is characteristic of the gaslike behavior. Especially, when the density is low enough, the interaction is essentially "binary" and τ_1^S can represent the interaction period. At 0.01 g cm^{-3}, the ratio τ_0^S / τ_1^S is as large as $\sim$5. As the bulk density is increased, τ_0^S / τ_1^S becomes $\sim$3 and $\sim$2 at 0.02 and 0.05 g cm^{-3}, respectively. It should be noted that the dilute-gas approximation in the simple gas kinetic theory requires stricter time scale separation that the time spent on free translation is much longer than that spent on binary collision. At a relatively low density of 0.01 g cm^{-3}, the free-translation period is only five times longer than the binary-interaction period.
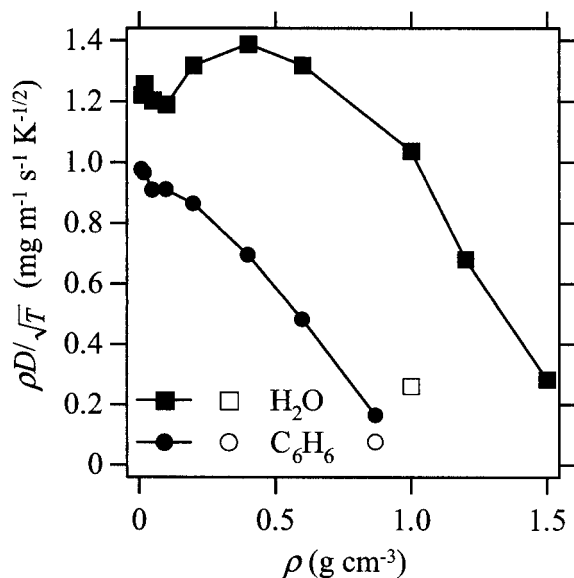
FIG. 3. The self-diffusion coefficients of water and benzene plotted against the density ρ in the form of the product $\rho D/\sqrt{T}$. The filled and open symbols represent $\rho D/\sqrt{T}$ at a supercritical temperature of 400 °C and at an ambient state, respectively.

In Fig. 2(c), we show τ_n^S(HB) conditioned by the number n_{HB} of hydrogen bonding.[61] In comparison to τ_n^S conditioned by the distance of the center of mass, the shell characterization by hydrogen bonding leads to the stronger control by the shell state and less by the bulk density. Since the orientational preference in attraction is essential in water, the shell state is conditioned more strongly by the number of hydrogen bonding that can distinguish the solvating molecules in the bonding configuration from those which are not.[62–64]

B. Translational dynamics

In the previous section, we have investigated the dynamics of the shell structure. In this section, we shed light on the translational diffusion process that sweeps in space. We show the dependence of the velocity relaxation on the shell state and establish the relationship to the mobility of the solvation shell.

In Fig. 3, we show the self-diffusion coefficients D obtained by the present MD simulation. The D values for water and benzene at 400 °C are shown against the density ρ in the form of the density-diffusivity product divided by the square root of the temperature, $\rho D/\sqrt{T}$. In supercritical conditions, especially at extremely low densities, it is more convenient to examine $\rho D/\sqrt{T}$ rather than D itself since D increases very steeply with density reduction. The product $\rho D/\sqrt{T}$ is independent of density in the case of the simplest kinetic model[11–13] at extremely low densities. The D values for water are in satisfactory agreement with those of experiment and TIP4P-FQ model calculation within 10%.[9,10] It is seen that $\rho D/\sqrt{T}$ for TIP4P water is relatively constant at 0.01–1.0 g cm^{-3}. In contrast, $\rho D/\sqrt{T}$ of benzene steeply decreases with increasing density as found in nonpolar supercritical fluids; cf. experimental results on methane,[65,66] ethylene,[67] xenon,[68] and carbon dioxide[69] and MD results on LJ fluid.[70] Thus, the increase in the diffusivity with decreas-

ing density is *exceptionally* small in the case of supercritical water. For water, $\rho D/\sqrt{T}$ decline is observed only above 1.0 g cm^{-3}. Actually, the packing fraction of water at the highest density of 1.5 g cm^{-3} (0.48) is comparable to that for benzene at 0.87 g cm^{-3} (0.51). The ambient density of 1.0 g cm^{-3} is not high enough for water since liquid water is known to have an open structure at 1.0 g cm^{-3} due to the hydrogen-bond network. The temperature dependence of D is much larger for water than for benzene when compared at their ambient densities: 1.0 and 0.87 g cm^{-3} for water and benzene, respectively. The difference comes from the difference in relaxation time τ_n^D, as shown below.

Now we examine the n and ρ dependencies of the conditional velocity relaxation time τ_n^D [Eq. (13)]; as described in Sec. II C, the locality in time of the relaxation process is measured by the relative strength of the n and ρ dependencies. As seen in Fig. 4(a), τ_n^D at fixed n increases with decreasing ρ and τ_n^D at fixed ρ increases with decreasing n. The presence of the ρ dependence at fixed n results from the commitment of the distant molecules to slow down the diffusion. The relaxation processes of velocity and solvation shell are correlated to a high degree in supercritical water, since the overall n dependencies of τ_n^D and τ_n^S are similar. The n dependence of τ_n^D is consistent with the dependence of the self-diffusion coefficient on the number of hydrogen bonds found by Marti *et al.* in their MD simulation along the coexistence curve using the flexible SPC model.[29]

In order to highlight the effect of hydrogen bonding, we compare τ_n^D for water with that for benzene. As shown in Fig. 4(b), τ_n^D for benzene is controlled more strongly by ρ and less by n than that for water. The self-diffusion in benzene is more nonlocal in time. Now we can explain the difference in the ρ dependence of D between supercritical water and benzene shown in Fig. 3 on the basis of the shell decomposition scheme. The general n and ρ dependencies of τ_n^D [Eq. (13)] and P_n [Eq. (4)] are summarized as follows: (1) τ_n^D at fixed n increases with decreasing ρ, (2) τ_n^D at fixed ρ increases with decreasing n, and (3) P_n distribution shifts to smaller n values with decreasing ρ.[71,72] The exceptionally weak ρ dependence of D for water comes from the two factors; the ρ dependencies of τ_n^D and P_n are smaller for water than for benzene. Although the larger n dependence of τ_n^D for water acts to increase the ρ dependence of D, this effect is overwhelmed by the former two factors. The ρ dependence of τ_n^D is useful for differentiating the diffusion of water and benzene, since diffusion sweeps in space and is determined not only by the in-shell relaxation but also by the relaxation outside the initial shell.

The temperature dependence of τ_n^D at the ambient density is much stronger for water than that for benzene due to the attractive interaction. The effect of attractive interaction is more strongly temperature dependent than the effect of repulsive interactions because of the difference in the potential steepness between the attractive and repulsive parts; recall that the quantity $\rho D/\sqrt{T}$ plotted in Fig. 3 is independent of temperature in the case of hard sphere model. The difference in τ_n^D dominates the difference in the observable diffusion coefficients D between water and benzene. The distribution mode of P_n shows smaller temperature dependence
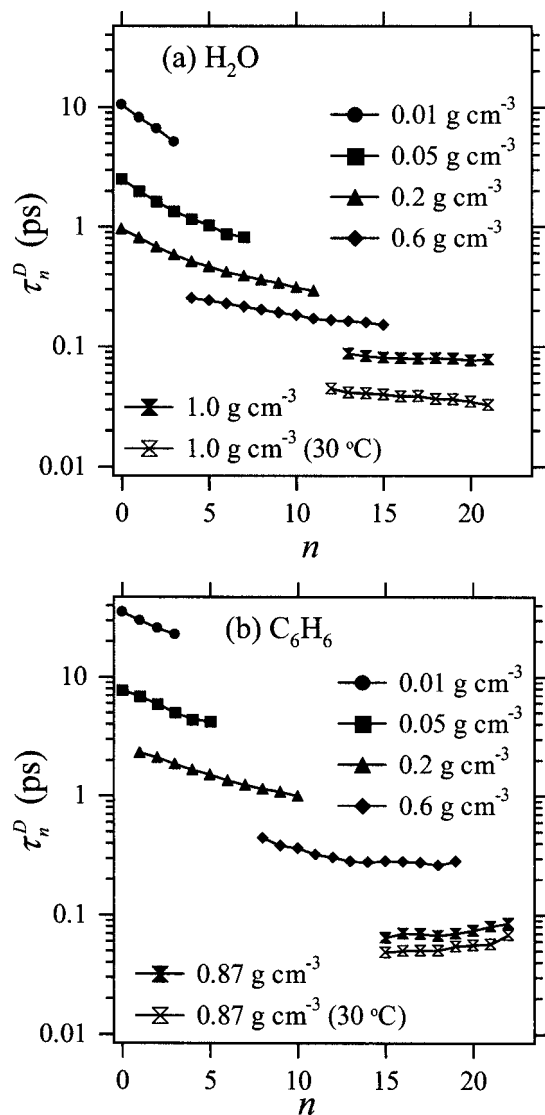
FIG. 4. The velocity autocorrelation time τ_n^D as a function of the solvation number n; (a) water at supercritical states of $0.01-1.0$ g cm^{-3} and 400 °C and at an ambient state of 1.0 g cm^{-3} and 30 °C and (b) benzene (OPLS-AA) at supercritical states of $0.01-0.87$ g cm^{-3} and 400 °C and at an ambient state of 0.87 g cm^{-3} and 30 °C. The filled and open symbols represent τ_n^D at a supercritical temperature of 400 °C and at an ambient state, respectively. For each n, the data at supercritical states correspond to the bulk densities of (a) $0.01-1.0$ g cm^{-3} and (b) $0.01-0.87$ g cm^{-3} from top to bottom.

FIG. 5. The ratio τ^D/τ^S plotted against the density ρ for water, benzene (OPLS-AA), and LJ. The filled and open symbols represent τ^D/τ^S at a supercritical temperature of 400 °C and at an ambient state, respectively.

than does τ_n^D, although the radial distribution function of water loses the three-dimensional network feature at elevated temperatures.[73,74]

Now we compare the translational velocity relaxation time τ^D with the solvation shell relaxation time τ^S in order to discuss whether the diffusion is of the in-shell type or of the mobile-shell type; for the physical meanings of in shell and mobile shell, see Sec. II C. The two extremes, $\tau^D/\tau^S \gg 1$ and $\tau^D/\tau^S \ll 1$, correspond to the dilute-gas-like picture and the dense liquidlike, Brownian picture, respectively. The ratio τ^D/τ^S for water in Fig. 5 shows that the water diffusion is of the mobile-shell type over the density range of $0.01-1.0$ g cm^{-3} at 400 °C.[75] At the ambient density of 1.0 g cm^{-3}, the packing fraction of water is still rather small (0.32) and the shell is mobile due to weakened hydrogen
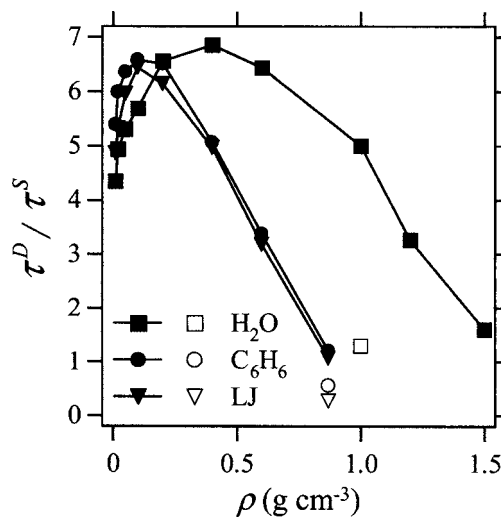
bonding at 400 °C. A large value of τ^D/τ^S at 1.0 g cm^{-3} and 400 °C means the invalidity of the liquidlike, Brownian picture and in favor of the gaslike picture. The collision (interaction) is, however, not binary. According to the P_n distribution in Fig. 1 and τ^D/τ^S in Fig. 5, the diffusing molecule is rather well solvated at densities of 0.05 g cm^{-3} and higher, but the solvation shell is too soft to allow the complete relaxation of the velocity within a shell even at 1.0 g cm^{-3}. The transition to the Brownian picture is seen only toward extremely compressed densities of $1.2-1.5$ g cm^{-3}.[76,77] At ambient temperature, τ^D/τ^S is much smaller than that at the same density at 400 °C and is comparable to unity. The shell is less mobile in ambient condition and the self-diffusion is of the in-shell type, in accordance with the Brownian picture.[78]

A remarkable contrast is seen between water and benzene in the density dependence of τ^D/τ^S at medium to high densities. As shown in Fig. 5, the ratio τ^D/τ^S for benzene is ~ 6 at 0.05 g cm^{-3} and decreases with density down to ~ 1 at the ambient density of 0.87 g cm^{-3}. In contrast to water, the benzene diffusion at 400 °C is of the mobile-shell type only in the low-density region and is of the in-shell type at the ambient density of 0.87 g cm^{-3}. This is in harmony with the common view of the transition from the collision to the Brownian picture with increasing density. Benzene is more highly packed at the ambient density and has smaller attractive interactions as well, and then the effect of repulsive interaction should be relatively stronger than that of water.

It is of interest to see if the difference in the ratio τ^D/τ^S between water and benzene can be attributed to the anisotropy of the potentials. For this purpose, we compare the LJ result with those for water and benzene. As seen from Fig. 5, the LJ results are similar to the OPLS-AA benzene results. The similarity indicates that benzene molecules can be considered to be freely rotating at a high temperature of 400 °C, as far as the translational dynamics is concerned.

We have seen that the velocity autocorrelation decays not only within the shell but also after the shell relaxation. In
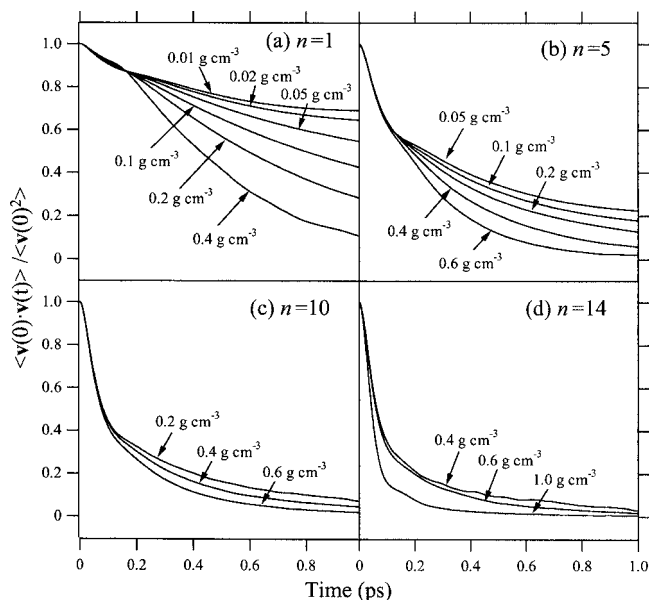
FIG. 6. The normalized velocity autocorrelation function of water at 400 °C for n=(a) 1, (b) 5, (c) 10, and (d) 14. The data correspond to the bulk densities of 0.01–1.0 g cm^{-3} from top to bottom. The data are absent at 0.01 g cm^{-3} for n=5, 10, and 14, at 0.02 g cm^{-3} for n=5, 10, and 14, at 0.05 g cm^{-3} for n=10 and 14, at 0.1 g cm^{-3} for n=10 and 14, at 0.2 g cm^{-3} for n=14, at 0.6 g cm^{-3} for n=1, at 1.0 g cm^{-3} for n=1, 5, and 10, and at 1.2 and 1.5 g cm^{-3} due to the negligible probabilities P_n for the corresponding n.

FIG. 7. The normalized velocity autocorrelation function of benzene at 400 °C for n=(a) 1, (b) 5, (c) 10, and (d) 14. The data correspond to the bulk densities of 0.01–0.87 g cm^{-3} from top to bottom. The data are absent at 0.01 g cm^{-3} for n=5, 10, and 14, at 0.02 g cm^{-3} for n=5, 10, and 14, at 0.05 g cm^{-3} for n=10 and 14, at 0.1 g cm^{-3} for n=10 and 14, at 0.4 g cm^{-3} for n=1, at 0.6 g cm^{-3} for n=1 and 5, and at 0.87 g cm^{-3} for n=1, 5, and 10 due to the negligible probabilities P_n for the corresponding n.

order to understand the velocity relaxation process within a shell and the effect of the cage-out on the velocity relaxation, we examine how the initial behavior of the velocity relaxation depends on the bulk density ρ and the solvation number n. First, we focus on the ρ dependence of the velocity autocorrelation functions with a fixed n value. Representative profiles for supercritical water are given in Fig. 6. It is seen that the initial decay for water up to 0.1 ps with a fixed n is independent of ρ in the low- to medium-density region of 0.01–0.6 g cm^{-3}. This clearly shows that the effect of the local structure on the self-diffusion up to ~0.1 ps is virtually independent of the bulk density and dominated by the initial solvation structure. Next, we focus on the n dependence of the velocity autocorrelation functions with a fixed ρ value. The initial decay of the velocity autocorrelation is faster for a larger n value. The initial decay is determined by the so-called Einstein frequency, which corresponds, on average, to the total force exerted on the diffusing molecule by the solvating molecules.[54] The present water results show that the total force exerted on the diffusing molecule is virtually determined by the solvating molecules within the first coordination shell, in agreement with the notion that the short-range, hydrogen-bonding interaction between neighboring molecules controls the diffusion process in supercritical water. Beyond 0.1 ps, the initial solvation structure is not the only factor determining the decay of the velocity autocorrelation function. The dependence on the bulk density ρ emerges. As a result, the time integral τ_n^D is dependent on ρ. The reorganization of the hydrogen bonding and the relaxation of the shell structure occur due to the exchange of the solvation shell states beyond 0.1 ps, which corresponds to the shell relaxation time.
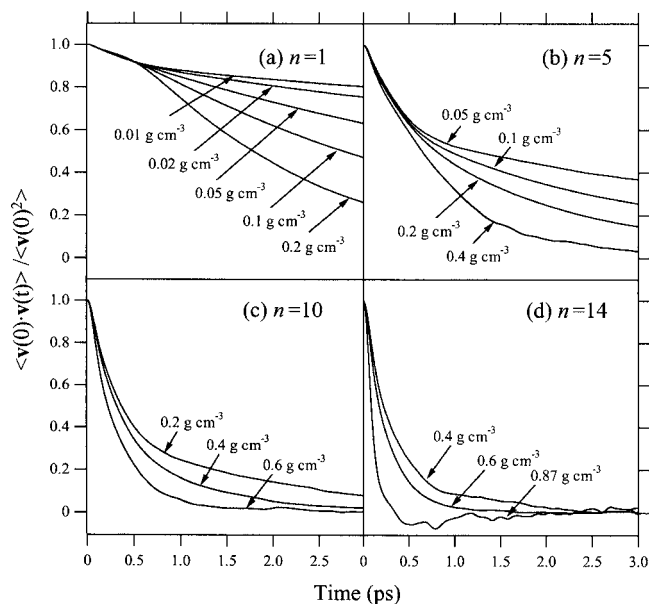
We can interpret the velocity relaxation profile on the basis of the time scale for the shell relaxation. For example, let us look at the relaxation profile for the solvation number n=5 at 0.05 g cm^{-3} in Fig. 6(b). At the bulk density of 0.05 g cm^{-3}, the monomers, dimers, and trimers are the majority [see Fig. 1(a)] and n=5 is a rare case. Up to 0.1 ps, the initial cage structure remains at n=5 and the forces from various directions reduce the velocity autocorrelation rapidly. Beyond 0.1 ps, the cage structure is relaxed, the water clusters are mainly disintegrated into monomers, dimers, and trimers, and the velocity relaxation becomes slower. Another example is the profile at n=1 at 0.4 g cm^{-3} in Fig. 6(a). Such an isolated condition of n=1 is rarely found at 0.4 g cm^{-3}. Beyond 0.1 ps, more water molecules cluster around and the velocity relaxation becomes faster.

The velocity relaxation profile for benzene is given in Fig. 7 in order to see its dependence on ρ and n. The short-time in-shell relaxation for benzene is more directly related to ρ than that for water; let us compare water in Fig. 6(c) and benzene in Fig. 7(c) at a typical value of n=10 in the density range of 0.2–0.6 g cm^{-3}. This difference between water and benzene corroborates the notion that the strong control by the shell states of the in-shell relaxation of water is attributed to the presence of the short-range, hydrogen-bonding interaction.

C. Rotational dynamics

To investigate the effect of hydrogen bonding on the dynamics in supercritical water, here we focus on the rotational dynamics. The rotational dynamics is a more powerful probe for the anisotropy in intermolecular potential.[46–48] We investigate the rotational dynamics in terms of the angular
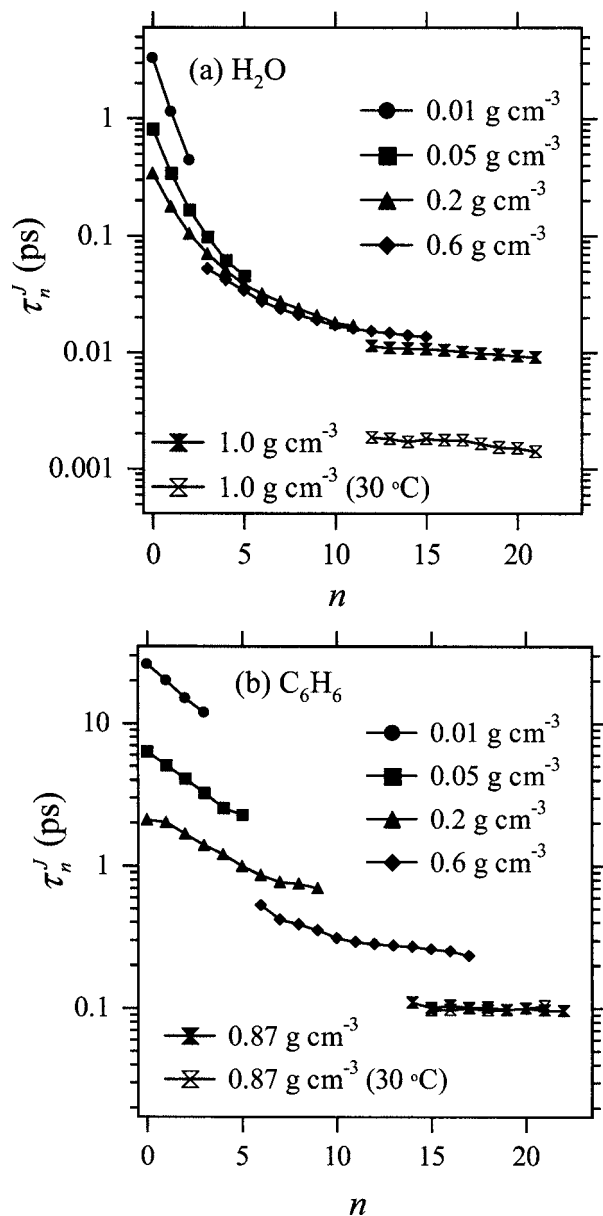
FIG. 8. The angular momentum correlation time τ_n^J as a function of the solvation number n; (a) water at supercritical states of $0.01-1.0$ g cm^{-3} and $400\,°C$ and at an ambient state of 1.0 g cm^{-3} and $30\,°C$ and (b) benzene (OPLS-AA) at supercritical states of $0.01-0.87$ g cm^{-3} and $400\,°C$ and at an ambient state of 0.87 g cm^{-3} and $30\,°C$. The filled and open symbols represent τ_n^J at a supercritical temperature of $400\,°C$ and at an ambient state, respectively.
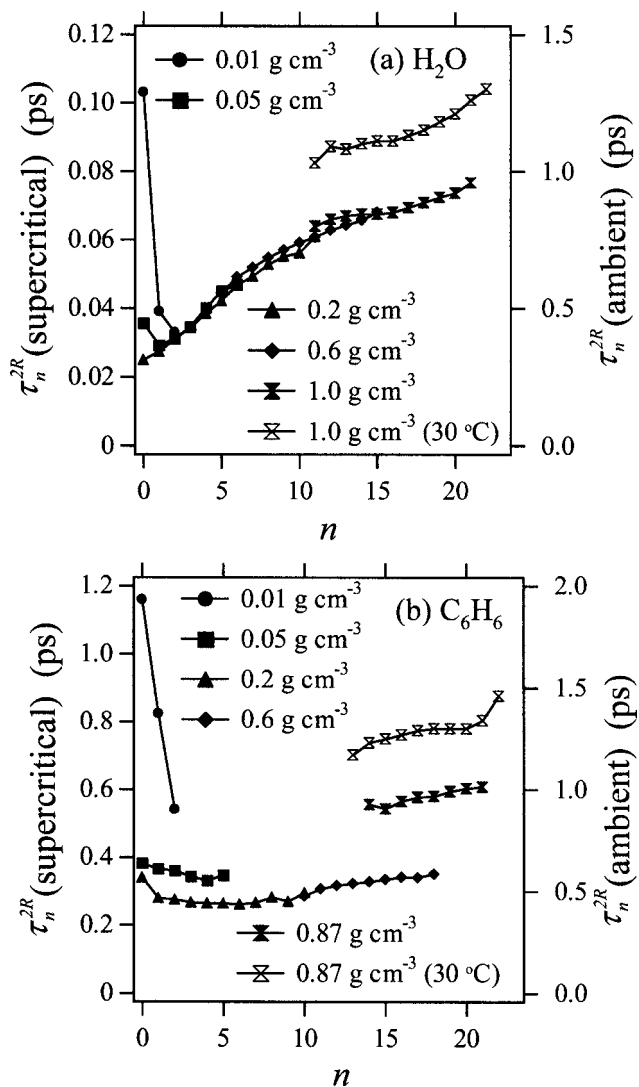

FIG. 9. The reorientational correlation time τ_n^{2R} as a function of the solvation number n; (a) water at supercritical states of $0.01-1.0$ g cm^{-3} and $400\,°C$ and at an ambient state of 1.0 g cm^{-3} and $30\,°C$ and (b) benzene (OPLS-AA) at supercritical states of $0.01-0.87$ g cm^{-3} and $400\,°C$ and at an ambient state of 0.87 g cm^{-3} and $30\,°C$. The filled and open symbols represent τ_n^{2R} at a supercritical temperature of $400\,°C$ and at an ambient state, respectively.

momentum correlation time τ^J and the second-rank reorientational correlation time τ^{2R}. τ^J is obtained from the trajectories in the (angular) momentum space and thus can be directly compared to τ^D. On the other hand, τ^{2R} has an advantage in comparison to the experiment since it can be directly compared to the NMR spin-lattice relaxation results.[8] It is also possible to compare τ^J with NMR spin-lattice relaxation results;[79] however, the analysis procedure for τ^J is more complicated and ambiguous than that for τ^{2R}.

First we show in Fig. 8(a) the angular momentum correlation time τ_n^J for water conditioned by the solvation number n. In comparison to τ_n^D, τ_n^J is much more strongly affected by n and less by ρ. This is because the rotational dynamics is of

the in-shell type as shown later. The rotational motion is more rapidly randomized by the directional hydrogen-bonding interaction. As seen in Fig. 8(b), benzene shows smaller dependence on the solvation number n and larger dependence on ρ than water. The difference in τ_n^J between water and benzene is more obvious than the difference in τ_n^D.

Now we inspect τ^{2R}. Figure 9(a) shows τ_n^{2R} for water. τ_n^{2R} is essentially independent of ρ when $n \geq 2$ and is controlled by the initial solvation structure, in agreement with Ref. 8. Similarly to the angular momentum relaxation, the orientational relaxation is of the in-shell type at $\lesssim 0.4$ g cm^{-3}, as shown below. τ_n^{2R} increases with n at $0.05-0.6$ g cm^{-3}, showing that a specific orientation of a water molecule is kept for a longer time when it is surrounded by a larger number of water molecules. In contrast to water, τ_n^{2R} for benzene in Fig. 9(b) is almost independent of n. The kinetic energy of rotation for the benzene molecule is large enough

to surmount its anisotropic potential at a high temperature of 400 °C, whereas the anisotropic attractive potential is strongly operative for water even at 400 °C. The temperature dependence of τ_n^{2R} is one order of magnitude larger for water than for benzene since the strongly anisotropic attractive interaction in water is more sensitive to the temperature variation. The reorganization of hydrogen bonds in water becomes much faster at a high temperature of 400 °C than in ambient condition, which makes the solvation shell rather mobile, as described in Sec. III B. Actually, a stronger response to the temperature variation has also been found for attractive interactions than for repulsive ones in thermodynamic analysis; the solvation free energy scaled by the thermal energy is a stronger function of temperature when the solute-solvent interaction is more polar.[80,81]

A few comments are made here on the reorientational relaxation. Since τ^{2R} probes the dynamics in the configuration space, the sign of the solvation-number and temperature dependencies of τ^{2R} is opposite to those of τ^D and τ^J. An increase in τ^{2R} for water at $n=0$ at $0.01-0.05$ g cm^{-3} and $n=1$ at 0.01 g cm^{-3} is due to the onset of the free-rotor-like character; τ^{2R} diverges in the zero-density limit because the angular momentum is conserved in the absence of the intermolecular interaction.[8,19,64] For benzene, the divergence behavior and the high-density behavior emerge at 0.05 and 0.87 g cm^{-3}, respectively.

Next we shall see if the rotational dynamics is of the in-shell type or not by using the ratios τ^J/τ^S and τ^{2R}/τ^S. The ratios τ^J/τ^S and τ^{2R}/τ^S are plotted against density ρ in Figs. 10(a) and 10(b), respectively. Both τ^J/τ^S and τ^{2R}/τ^S for water are comparable to and smaller than unity at 0.6 g cm^{-3} and lower, showing that the rotational dynamics is of the in-shell type in low- to medium-density supercritical water. In other words, the solvating molecules are exchanged by hydrogen-bonding reorganization, in correspondence to the rotational relaxation. The ratio τ^J/τ^S as well as τ^D/τ^S for water is relatively constant over the wide range of density of $0.01-1.0$ g cm^{-3}. On the other hand, the ratio τ^{2R}/τ^S increases with density, indicating that a water molecule can exchange the hydrogen-bonding partner more easily at a higher density. A similar property has been seen in the energetic analysis that the change in the total internal energy upon formation or breakage in a specific hydrogen bonding is smaller at a higher density.[18]

The effect of the anisotropic hydrogen bonding is clearly seen in comparison to benzene. The ratio τ^J/τ^S for benzene shown in Fig. 10(a) is 3–5 at $0.05-0.6$ g cm^{-3}, which is much larger than that for water. The rotation of benzene is of the mobile-shell type, in contrast to the in-shell-type rotation of water. τ^{2R}/τ^S for benzene is also larger than that for water at 400 °C at $0.01-1.0$ g cm^{-3}. Due to the absence of the hydrogen bonding, it is easier for a benzene molecule than for a water molecule to exchange the solvating molecules without changing its orientation. This is consistent with the recent trajectory analysis of supercritical fluid by Sato and Okazaki.[82] They have shown that a polar solvent continuously interacts with polar solute while the interaction between nonpolar solute and nonpolar solvent is pulselike. The orientational relaxation for water is much more sensitive to
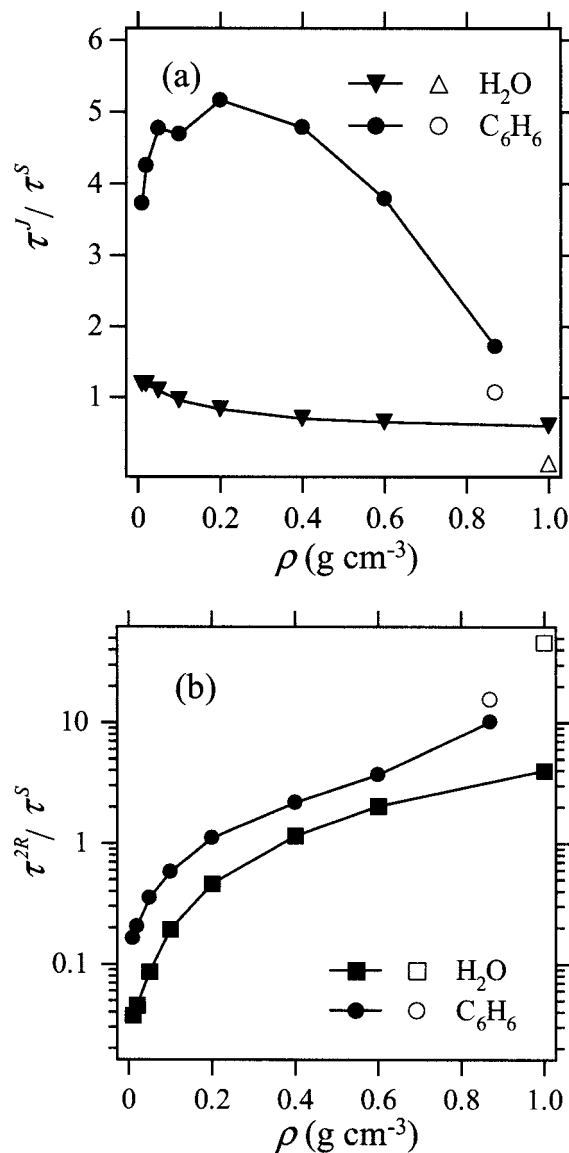

FIG. 10. The ratios (a) τ^J/τ^S and (b) τ^{2R}/τ^S plotted against the density ρ for water and benzene. The filled and open symbols represent τ^J/τ^S and τ^{2R}/τ^S at a supercritical temperature of 400 °C and at an ambient state, respectively.

the temperature variation than the shell relaxation due to the anisotropy of the hydrogen bonding.[83] In the case of benzene, the difference in the temperature dependence between orientational relaxation and shell relaxation is much smaller.[84]

IV. CONCLUSIONS

The relationship among the solvation shell dynamics, translational dynamics, and rotational dynamics in supercritical water has been examined over the wide density range of $0.01-1.5$ g cm^{-3} and in the ambient condition. The time scales of dynamics in supercritical water in the low- to medium-density range of $0.05-0.4$ g cm^{-3} are in the following sequence:

$$\tau_n^D > \tau_n^S \gtrsim \tau_n^{D,i} \gtrsim \tau_n^J \gtrsim \tau_n^{2R}, \qquad (16)$$

where $\tau_n^{D,i}$ is the initial period of the velocity relaxation during which the velocity autocorrelation function with fixed n does not depend on the bulk density. The self-diffusion is of the mobile-shell type, while the rotation is of the in-shell type. This sequence is different from that in the ambient conditions $(\tau_n^{2R} > \tau_n^S \simeq \tau_n^D \gtrsim \tau_n^J)$ and is in disagreement with the Brownian picture. Moreover, the distribution mode of the probability P_n shows that the binary collision picture is not applicable at $\gtrsim 0.05$ g cm^{-3}. Thus, the present shell decomposition scheme negates the simplified, collision and Brownian pictures and provides the following realistic picture.

First a water molecule changes the orientation to break hydrogen bonding. After the breakage of one or two hydrogen bonds, the shell structure is relaxed. Until then, the diffusion is controlled by the initial shell structure. After the shell relaxation, the solvating molecules are reconstructed and the diffusion is controlled by the averaged shell state rather than the conditional shell state at time 0. This shell relaxation is repeated several times so that the water molecule may completely lose the velocity time correlation. The present physical picture will be valuable for understanding the mechanism of reaction dynamics in supercritical water.

Let us summarize the density dependencies of τ^D, τ^J, τ^{2R}, and τ^S. It has been found that τ^D, τ^J, and τ^S increase and τ^{2R} decreases with density reduction. The density dependence of τ^{2R} is much smaller than those of τ^D, τ^J, and τ^S; the changes in τ^{2R} are only $\sim 40\%$ and $\sim 10\%$ for water and benzene, respectively, in response to the density reduction from 0.6 to 0.1 g cm^{-3} at a fixed temperature of 400 °C, whereas τ^D, τ^J, and τ^S at 0.1 g cm^{-3} are 5–11 times larger than those at 0.6 g cm^{-3}. The density dependencies of τ^D, τ^J, and τ^S come both from the density dependence of relaxation times at a fixed n and the shift in the probability P_n of the occurrence of n. The density dependencies of τ^J and τ^{2R} are primarily due to the shift in P_n and, further, the n dependence of τ^{2R} is smaller than those of τ^D, τ^J, and τ^S. As a result, the density dependence of τ^{2R}/τ^S is one order of magnitude larger than those of τ^D/τ^S and τ^J/τ^S.

The water results are further compared to the benzene results at 400 °C and at 0.01–0.87 g cm^{-3} and in the ambient condition to see the effect of hydrogen bonding. The effects of hydrogen bonding are summarized as follows:

(1) The density dependence of the self-diffusion coefficient is smaller for water.

(2) The temperature dependence of the self-diffusion coefficient at a density fixed at the ambient value, 1.0 g cm^{-3} for water and 0.87 g cm^{-3} for benzene, is much larger for water.

(3) The transition from collision picture to Brownian picture with increasing density is not seen for supercritical water up to the ambient density, whereas such transition is seen for benzene.

(4) The dependence of rotational dynamics on the shell structure is larger for water.

(5) The rotational relaxation for water is of the in-shell type, whereas that for benzene is of the mobile-shell type.

These differences are dynamical manifestations of the anisotropy of the intermolecular interactions.

ACKNOWLEDGMENTS

[1] *Water, A Comprehensive Treatise*, edited by F. Franks (Plenum, New York, 1972), Vol. 1; (Plenum, New York, 1973), Vol. 2; (Plenum, New York, 1973), Vol. 3; (Plenum, New York, 1975), Vol. 4; (Plenum, New York, 1975), Vol. 5; (Plenum, New York, 1979), Vol. 6; (Plenum, New York, 1982), Vol. 7.

[2] J. S. Seewald, Nature (London) **370**, 285 (1994).

[3] P. A. Marrone, T. A. Arias, W. A. Peters, and J. W. Tester, J. Phys. Chem. A **102**, 7013 (1998).

[4] N. Akiya and P. E. Savage, Chem. Rev. (Washington, D.C.) **102**, 2725 (2002); J. T. Henrikson, C. R. Grice, and P. E. Savage, J. Phys. Chem. A **110**, 3627 (2006).

[5] J. M. DeSimone, Science **297**, 799 (2002).

[6] D. Miksa, J. Li, and T. B. Brill, J. Phys. Chem. B **106**, 11107 (2002).

[7] Y. Yasaka, K. Yoshida, C. Wakai, N. Matubayasi, and M. Nakahara, J. Phys. Chem. A **110**, 11082 (2006).

[8] N. Matubayasi, N. Nakao, and M. Nakahara, J. Chem. Phys. **114**, 4107 (2000).

[9] K. Yoshida, C. Wakai, N. Matubayasi, and M. Nakahara, J. Chem. Phys. **123**, 164506 (2005).

[10] K. Yoshida, N. Matubayasi, and M. Nakahara, J. Chem. Phys. **125**, 074307 (2006); **126**, 089901 (2007).

[11] J. O. Hirschfelder, C. F. Curtiss, and R. B. Bird, *Molecular Theory of Gases and Liquids* (Wiley, New York, 1954).

[12] S. Chapman and T. G. Cowling, *The Mathematical Theory of Non-Uniform Gases*, 3rd ed. (Cambridge University Press, London, 1970).

[13] D. A. McQuarrie, *Statistical Mechanics* (Harper & Row, New York, 1976).

[14] C. Wakai and M. Nakahara, J. Chem. Phys. **106**, 7512 (1997).

[15] H. J. V. Tyrrell and K. R. Harris, *Diffusion in Liquids* (Butterworths, London, 1984).

[16] H. J. C. Berendsen, J. R. Grigera, and T. P. Straatsma, J. Phys. Chem. **91**, 6269 (1987).

[17] L. X. Dang, J. Chem. Phys. **97**, 2659 (1992).

[18] N. Matubayasi, C. Wakai, and M. Nakahara, J. Chem. Phys. **107**, 9133 (1997).

[19] N. Yoshii, H. Yoshie, S. Miura, and S. Okazaki, J. Chem. Phys. **109**, 4873 (1998).

[20] P. B. Balbuena, K. P. Johnston, P. J. Rossky, and J. K. Hyun, J. Phys. Chem. B **102**, 3806 (1998).

[21] N. Matubayasi, C. Wakai, and M. Nakahara, J. Chem. Phys. **110**, 8000 (1999).

[22] A. A. Chivalo and P. T. Cummings, Adv. Chem. Phys. **109**, 115 (1999).

[23] M. S. Skaf and D. Laria, J. Chem. Phys. **113**, 3499 (2000).

[24] C.-N. Yang and H. J. Kim, J. Chem. Phys. **113**, 6025 (2000).

[25] Y. Danten, T. Tassaing, and M. Besnard, J. Chem. Phys. **123**, 074505 (2005).

[26] We use the term shell or cage to refer to the collection of the solvating molecules, as defined in Sec. II B, although a low density of 0.01 g cm^{-3} is included.

[27] M. Ferrario, M. Haughney, I. R. McDonald, and M. L. Klein, J. Chem. Phys. **93**, 5156 (1990).

[28] A. Luzar and D. Chandler, Nature (London) **379**, 55 (1996); Phys. Rev. Lett. **76**, 928 (1996).

[29] J. Marti, J. A. Padro, and E. Guàrdia, J. Chem. Phys. **105**, 639 (1996).

[30] J. Marti, Phys. Rev. E **61**, 449 (2000).

[31] B. S. Mallik and A. Chandra, J. Chem. Phys. **125**, 234502 (2006).

[32] A. S. Quist and W. L. Marshall, J. Phys. Chem. **72**, 684 (1968).

[33] A. Ebertz and E. U. Franck, Ber. Bunsenges. Phys. Chem. **99**, 1091 (1995).

[34] P. B. Balbuena, K. P. Johnston, P. J. Rossky, and J. K. Hyun, J. Phys. Chem. B **102**, 3806 (1998).

[35] K. Okada, M. Yao, Y. Hiejima, H. Kohno, and Y. Kajihara, J. Chem. Phys. **110**, 3026 (1999).

[36] P. C. Ho, H. Bianchi, D. A. Palmer, and R. H. Wood, J. Solution Chem. **29**, 217 (2000).

[37] T. Tassaing and M.-C. Bellissent-Funel, J. Chem. Phys. **113**, 3332 (2000).

[38] T. Ohmori and Y. Kimura, J. Chem. Phys. **119**, 7328 (2003).

[39] T. Hoshina, N. Tsuchihashi, K. Ibuki, and M. Ueno, J. Chem. Phys. **120**, 4355 (2004).

[40] L. Hnedkovsky, R. H. Wood, and V. N. Balashov, J. Phys. Chem. B **109**, 9034 (2005).

[41] M. Nakahara, *Proceedings of the 14th International Conference on the Properties of Water and Steam, Kyoto, Japan, 2004*, edited by M. Nakahara, N. Matubayasi, M. Ueno, K. Yasuoka, and K. Watanabe (Maruzen, Tokyo 2005), p. 12.

[42] H. Weingärtner and E. U. Franck, Angew. Chem., Int. Ed. **44**, 2672 (2005).

[43] N. Kometani, S. Arzhantsev, and M. Maroncelli, J. Phys. Chem. A **110**, 3405 (2006).

[44] A. Laaksonen, P. Stilbs, and R. E. Wasylishen, J. Chem. Phys. **108**, 455 (1998).

[45] T. Tassaing, M. I. Cabaço, Y. Danten, and M. Besnard, J. Chem. Phys. **113**, 3757 (2000).

[46] C. Wakai and M. Nakahara, J. Chem. Phys. **103**, 2025 (1995).

[47] M. Nakahara, C. Wakai, Y. Yoshimoto, and N. Matubayasi, J. Phys. Chem. **100**, 1345 (1996).

[48] Y. Yasaka, C. Wakai, N. Matubayasi, and M. Nakahara, J. Phys. Chem. A **111**, 541 (2007).

[49] Release on the IAPWS Formulation 1995 for the Thermodynamic Properties of Ordinary Water Substances for General and Scientific Use (http://www.iapws.org).

[50] R. D. Goodwin, J. Phys. Chem. Ref. Data **17**, 1541 (1988).

[51] R. C. Reid, J. M. Prausnitz, and B. E. Poling, *The Properties of Gases and Liquids*, 4th ed. (McGraw-Hill, New York, 1987).

[52] W. L. Jorgensen, J. Chandrasekhar, and J. D. Madura, J. Chem. Phys. **79**, 926 (1983).

[53] W. L. Jorgensen and D. L. Severance, J. Am. Chem. Soc. **112**, 4768 (1990).

[54] J. P. Hansen and I. R. McDonald, *Theory of Simple Liquids* (Academic, London, 1986).

[55] M. P. Allen and D. J. Tildesley, *Computer Simulation of Liquids* (Oxford University Press, Oxford, 1987).

[56] Since the potentials used in the present study are smooth, collision cannot be defined so clearly as in the case of hard sphere model. Thus it is more appropriate to use the terms "interaction period." Nevertheless, we also use the term "collision" since this term is well known in textbooks.

[57] N. Matubayasi, L. H. Reed, and R. M. Levy, J. Phys. Chem. **98**, 10640 (1994).

[58] N. Matubayasi and R. M. Levy, J. Phys. Chem. **100**, 2681 (1996).

[59] N. Matubayasi, E. Gallicchio, and R. M. Levy, J. Chem. Phys. **109**, 4864 (1998).

[60] Since P_n at $N \geq 2$ accounts for a large fraction at 0.05 g cm^{-3}, supercritical water reactions in such low-density region are not of gas-phase type and are affected by the solvation.

[61] In the case of τ_n^S(HB), the $C_n(t)$ data were fitted before they become less than 0.95 for $n_{HB}=0$ at 0.05–0.1 g cm^{-3}, before they become less than 0.9 for $n_{HB}=0$ at 0.2 g cm^{-3}, and before they become less than 0.8 for

$n_{HB}=1$ at 0.05, 0.1, and 0.2 g cm^{-3} due to the high probability P_n of occurrence at those conditions. It was impossible to obtain τ_n^S(HB) at 0.01 and 0.02 g cm^{-3} since P_0 was too high. At the higher densities, we used the $C_n(t)$ data before they become less than 0.7, as in the case of τ_n^S conditioned by the solvation number n.

[62] It is of interest to comment on the relationship of the present shell relaxation time τ^S to the "residence time" (see, for example, Refs. 63 and 64). The shell relaxation time τ^S reflects the rate of transition between the states of the solvation shell of a specific solute molecule, whereas the residence time reflects the relaxation of the intermolecular distance between a solute and a certain solvent molecule. Thus the shell relaxation time is a collective property of solvating molecules, whereas the residence time is a property of a pair of molecules. In this work, we examine the former one in order to focus on the relationship of solvation shell relaxation to single-molecular processes of translational and rotational relaxations. The previous MD study on supercritical water (Ref. 64) has shown that the residence time is relatively constant at 0.2–0.7 g cm^{-3}, in contrast to the decrease in τ^S with increasing density in the corresponding density region. These findings show that at higher densities, where the solvation number is larger, the states of the solvation shell relax with exchanging only the small portion of the solvating molecules and the good portion of the solvent molecules are resident during the shell-state relaxation.

[63] L. W. Flanagin, P. B. Balbuena, K. P. Johnston, and P. J. Rossky, J. Phys. Chem. **99**, 5196 (1995).

[64] E. Guardia and J. Marti, Phys. Rev. E **69**, 011502 (2004).

[65] P. H. Oosting and N. J. Trappeniers, Physica (Amsterdam) **51**, 418 (1971).

[66] K. R. Harris, Physica A **94**, 448 (1978).

[67] B. Arends, K. O. Prins, and N. J. Trappeniers, Physica A **107**, 307 (1981).

[68] P. W. E. Peereboom, H. Luigjes, and K. O. Prins, Physica A **156**, 260 (1989).

[69] P. Etesse, J. A. Zega, and R. Kobayashi, J. Chem. Phys. **97**, 2022 (1992).

[70] K. Meier, A. Laesecke, and S. Kabelac, J. Chem. Phys. **121**, 9526 (2004).

[71] Since the P_n distribution shifts to smaller n values with decreasing ρ, τ^D increases with decreasing ρ, according to the sum rule in Eq. (13). No anomaly, such as nonmonotonic behavior, can arise in the density dependence of τ^D even in the vicinity of the critical density at 400 °C, contrary to the previous discussion in Ref. 72.

[72] A. N. Drozdov and S. C. Tucker, J. Chem. Phys. **114**, 4912 (2001).

[73] R. D. Mountain, J. Chem. Phys. **90**, 1866 (1989).

[74] N. Matubayasi and M. Nakahara, J. Chem. Phys. **112**, 8089 (2000).

[75] The decrease in τ^D/τ^S is seen in the extremely low-density region. This is because the free-translation period τ_0^S, which is very large in the extremely low-density region as mentioned in Sec. III A, is included in τ^S. When the density is extremely low, it will be insightful to further decompose τ_0^S to examine, for example, the effect of orbiting within the attractive hydrogen-bonding potential.

[76] Water is in the liquid phase at 1.5 g cm^{-3} and below (Ref. 77). Indeed, D changes without orders of magnitude variation and the profile of radial distribution function shows disordered, liquidlike behavior up to 1.5 g cm^{-3} (data not shown). The experimental pressure values for water at 400 °C are 2.0×10^3 and 6.2×10^3 MPa at 1.2 and 1.5 g cm^{-3}, respectively (Ref. 49).

[77] W. Wagner and A. Pruß, J. Phys. Chem. Ref. Data **31**, 387 (2002).

[78] The discussions above are not changed when τ^S(HB), which is the shell relaxation time conditioned by the number of hydrogen bonding, is used instead of τ^S.

[79] W. J. Lamb and J. Jonas, J. Chem. Phys. **74**, 913 (1981).

[80] N. Matubayasi and M. Nakahara, J. Chem. Phys. **117**, 3605 (2002); **118**, 2446 (2003).

[81] N. Matubayasi and M. Nakahara, J. Chem. Phys. **122**, 074509 (2005).

[82] M. Sato and S. Okazaki, J. Chem. Phys. **123**, 124508 (2005); **123**, 124509 (2005).

[83] The discussion above is not changed if the shell state is conditioned in terms of the number of hydrogen bonds instead of the solvation number. The ratios τ^I/τ^S(HB) and τ^{2R}/τ^S(HB) depend on density and temperature in similar ways to τ^I/τ^S and τ^{2R}/τ^S, respectively, where τ^S(HB) is the shell relaxation time in which the shell state is conditioned by the number of hydrogen bonds.

[84] We have investigated the rotational dynamics in terms of the second-rank

reorientational relaxation time τ^{2R} for the sake of comparison to the previous NMR results (Ref. 8). We also examined the first-rank reorientational relaxation time τ^{1R}, which is defined as $\tau^{1R} = \int_0^\infty dt \langle \cos \theta(t) \rangle$. Similarly to τ_n^{2R}, τ_n^{1R} for water conditioned by the solvation number n is larger at a larger value of n and weakly dependent on the bulk density ρ. The τ_n^{1R} values are twice as large as the τ_n^{2R} values at corresponding n and ρ, in agreement with the existence of the preference of the hydrogen-bonding angle (Ref. 21). The τ_n^{1R} values for benzene is almost equal to the τ_n^{2R} values at corresponding n and ρ, showing that benzene molecules rotate more freely.